Radiochim. Acta **90**, 147–153 (2002)

Study of uranyl(VI) malonate complexation by time resolved laser-induced fluorescence spectroscopy (TRLFS)

By A. Brachmann[1], G. Geipel[2], G. Bernhard[2] and H. Nitsche[3,*]

[1] Stanford Linear Accelerator Center, P.O. Box 4349, MS 66, Stanford, CA 94309, USA
[2] Forschungszentrum Rossendorf e.V., Institute of Radiochemistry, P.O. Box 510119, D-01314 Dresden, Germany
[3] University of California at Berkeley, Department of Chemistry, and The Glenn T. Seaborg Center, Lawrence Berkeley National Laboratory, Cyclotron Road, MS 70A-1150, Berkeley, CA 94720, USA

(Received August 30, 1999; accepted in final form October 2, 2001)

Time resolved fluorescence / Uranyl(VI) ion / Complexation / Malonic acid / Uranyl(VI) malonate

Summary. The uranyl(VI) malonate complex formation was studied by time-resolved laser-induced fluorescence spectroscopy (TRLFS) at pH 4 and an ionic strength of 0.1 M $NaClO_4$. The uranium concentration was 5×10^{-6} M at ligand concentrations from 1×10^{-5} to 1×10^{-2} M.

The measured fluorescence lifetimes of the 1 : 1 and 1 : 2 uranyl(VI) malonate complexes are 1.24 ± 0.02 μs and 6.48 ± 0.02 μs, respectively. The fluorescence lifetime of the uranyl(VI) ion is 1.57 ± 0.06 μs in 0.1 M perchloric media. The main fluorescence bands of the malonate complexes show a bathochromic shift compared to the uranyl(VI) ion and are centered at 494 nm, 515 nm and 540 nm for the 1 : 1 complexes and at 496 nm, 517 nm and 542 nm for the 1 : 2 complex. The spectra of the individual uranyl(VI) malonate complexes were calculated using a multi exponential fluorescence decay function for each intensity value at each wavelength, covering the entire wavelength range. Stability constants were determined for the complexes $UO_2C_3H_2O_4^{\circ}{}_{(aq)}$ and $UO_2(C_3H_2O_4)_2^{2-}$ from results of spectra deconvolution using a least square fit algorithm ($\log \beta_1^{\circ} = 4.48 \pm 0.06$, $\log \beta_2^{\circ} = 7.42 \pm 0.06$ or $\log K_2^{\circ} = 2.94 \pm 0.04$). The results are compared with literature values obtained by potentiometric measurements.

1. Introduction

The complexation behavior of humic substances with uranyl(VI) ions has been studied extensively [1–10]. Humic substances are complex polyelectrolytes. Their thermodynamic descriptions include the metal ion charge neutralization model proposed by Czerwinski *et al*. [1] and the approach using protonation capacities of functional groups published by Rao and Choppin [10].

In order to simulate humic acid functionality, we used model substances with elementary structural units of humic acid molecules for thermodynamic studies of their metal ion complexation behavior. The functional elements of humic substances involved in the complexation of metal ions are mainly carboxylic and phenolic groups [11–15]. However, the dissociation of phenolic groups occurs mostly at alkaline pH. Our experiments were carried out at a pH of 4 to minimize hydrolysis of the uranyl(VI) ion. At this pH only the interaction with the carboxylic groups has to be considered.

Our functional model substances are mono- and dicarboxylic acids such as salicylic, phthalic and malonic acid. Salicylic and phthalic acids represent simple aromatic structural elements of a typical humic acid molecule. Malonic acid can serve as an aliphatic structural element.

The interaction of the uranyl(VI) ion with carboxylic acids was studied by several authors [15–22]. However, most of these studies used indirect determination methods such as potentiometric titrations. All reported investigations required uranium concentrations of 10^{-2} to 10^{-4} M, which is much above the concentration levels usually found in uranium-contaminated environments.

This paper presents a direct study of uranyl(VI) malonate complexation using laser-induced time-resolved fluorescence spectroscopy at metal concentrations relevant for environmental aquatic systems.

2. Experimental

2.1 Reagents

All chemicals were purity grade "pro analysis, p.a." (Merck). Filtered and deionized water (Milli-RO, Milli-Q-System, Millipore, Molsheim, France) was used for sample preparation. The uranium stock solution was prepared by dissolving $Na_2U_2O_7 \cdot 6H_2O$ in 1 M $HClO_4$ (Sodium diuranate hexahydrate was precipitated from uranyl nitrate solution according to the method given by Gmelin [23]).

Weighed amounts of malonic acid were dissolved in water to prepare two stock solutions of 10^{-3} M and 5×10^{-5} M each. The elemental composition of the malonic acid was verified with an elemental analyzer (Model CHNF-932, Leco, St. Joseph, MI, USA). The purity of the chemicals and the analytical uranium concentration of the uranium stock solution was determined by ICP-MS analysis.

Aliquots were transferred into volumetric flasks to obtain a final uranium concentration of 5×10^{-6} M. For each sample, the malonic acid stock solution was added to cover a metal : ligand ratio range from 1 : 2 to 1 : 2000.

*Author for correspondence (E-mail: HNitsche@lbl.gov).

Table 1. Species concentrations and stability constants obtained in this work ($\log\beta$ values for samples 11–14 are not calculated due to insignificant concentrations of $UO_2^{2+}{}_{(free)}$) ($^*\log\beta_{2\,I=0.1\ M} = \log\beta_{1,\,I=0.1\ M} + \log K_{2,\,I=0.1\ M}$).

No.	$C_3H_{4-x}O_4^{-x}{}_{(tot.)}$ [M]	$C_3H_2O_4^{2-}$ [M]	$UO_2^{2+}{}_{(free)}$ [M]	$UO_2C_3H_2O_4^{\circ}{}_{(aq)}$ [M]	$UO_2(C_3H_2O_4)_2^{2-}$ [M]	$\log\beta_{1,\,I=0.1\ M}$ ($\pm$0.02)	$\log\beta_{2,\,I=0.1\ M}$ ($\pm$0.04)	$\log K_{2,I=0.1\ M}$ ($\pm$0.04)
1	0	0	5.00×10^{-6}	0	0	–	–	–
2	1.0×10^{-5}	5.03×10^{-7}	4.42×10^{-6}	6.84×10^{-7}	–	5.49	–	–
3	2.5×10^{-5}	1.28×10^{-6}	3.75×10^{-6}	1.37×10^{-6}	–	5.46	–	–
4	5.0×10^{-5}	2.59×10^{-6}	3.14×10^{-6}	1.93×10^{-6}	–	5.38	9.18*	3.80
5	7.5×10^{-5}	3.92×10^{-6}	2.66×10^{-6}	2.39×10^{-6}	–	5.36	9.21*	3.85
6	1.0×10^{-4}	5.24×10^{-6}	2.31×10^{-6}	2.82×10^{-6}	1.40×10^{-7}	5.37	9.35	3.98
7	2.5×10^{-4}	1.33×10^{-5}	1.33×10^{-6}	3.29×10^{-6}	3.70×10^{-7}	5.27	9.20	3.93
8	5.0×10^{-4}	2.67×10^{-5}	6.04×10^{-7}	3.48×10^{-6}	7.35×10^{-7}	5.33	9.23	3.90
9	7.5×10^{-4}	4.02×10^{-5}	5.10×10^{-7}	3.53×10^{-6}	9.88×10^{-7}	5.24	9.08	3.84
10	1.0×10^{-3}	5.37×10^{-5}	3.11×10^{-7}	3.38×10^{-6}	1.22×10^{-6}	5.31	9.14	3.83
11	2.5×10^{-3}	1.35×10^{-4}	–	2.61×10^{-6}	2.41×10^{-6}	–	–	3.84
12	5.0×10^{-3}	2.70×10^{-4}	–	1.78×10^{-6}	3.17×10^{-6}	–	–	3.82
13	7.5×10^{-3}	4.05×10^{-4}	–	1.37×10^{-6}	3.58×10^{-6}	–	–	3.81
14	1.0×10^{-2}	5.40×10^{-4}	–	1.06×10^{-6}	3.85×10^{-6}	–	–	3.83

Diluted $HClO_4$ and NaOH were used to adjust the sample pH to 4. The ionic strength of the solutions was 0.1 M ($NaClO_4$). After preparation, the samples were transferred into polyethylen vials (Packard Instruments B.V., Groningen, The Netherlands) and placed on an automatic agitator for 24 h. Before measurements were conducted, the pH value was checked again and adjusted if necessary. A pH micro-electrode (U 402-M6-S7, Ingold Meßtechnik GmbH, Steinbach, Germany) was used for pH measurements.

Additionally, samples with varied uranium concentrations in 0.1 M perchloric acid were prepared to check the linearity of uranyl(VI) fluorescence intensity as a function of concentration. Table 1 summarizes the composition of the investigated samples.

2.2 Time-resolved laser induced fluorescence spectroscopy

The time-resolved laser-induced fluorescence experiments were performed with a Nd:YAG laser (GCR 230, Spectra Physics, USA). For fluorescence excitation the fourth harmonic wavelength (266 nm) of the Nd:YAG laser was used, which is generated by an external frequency doubling unit. To prevent photolytical degradation of the organic ligand, the pulse intensity was restricted to about 1 mJ. Time-resolved mode was used to obtain fluorescence decay spectra and to discriminate the fluorescence signal against the laser pulse. A detailed description of the experimental setup is given by Geipel *et al.* [24]. Spectra were recorded in 1 µs time steps starting from 0.2 µs after the laser pulse. Fluorescence spectra were collected from 600 laser shots for every single delay time.

2.3 Determination of fluorescence lifetimes and deconvolution of emission spectra

To obtain the fluorescence lifetime constants of the involved species, the spectra were analyzed with the program "POLYLIFE", developed in our group. A detailed description of the program is given by Brendler *et al.* [25]. The general approach is to fit the fluorescence lifetime constants and fluorescence yields as a function of the wavelength according to the fluorescence decay equation:

$$A_{I,\mathrm{a,total}} = \sum_{a=1}^{b} A_{I,t_0,a}\,\mathrm{e}^{-\frac{t}{\tau_a}} \qquad (1)$$

with A: integral fluorescence intensity of species 'a' for the wavelength value I at time t for gating time (1 µs); t: time after fluorescence excitation, a: number of fluorescent species, τ_a: fluorescence lifetime constant of species a.

The separate fit of fluorescence lifetime parameters for each wavelength value allows the decomposition of superimposed single-species spectra. All spectra of one time-resolved measurement were combined into a matrix which was processed by the program. The fluorescence decay constants were determined restricting the evaluated wavelength range from 500 nm to 550 nm in order to avoid the influence of the lower signal-to-noise ratio at the beginning and end of the spectra. In a second fitting step, the mean fluorescence decay constants were held constant but the wavelength range was extended to cover the full range of the emission spectra (450 nm–630 nm). The results are the mean fluorescence decay constants and the single species fluorescence contributions.

In addition to the single component uranyl(VI) malonate spectra obtained by the POLYLIFE fit procedure, the spectrum of the uranyl(VI) ion in 0.1 M perchloric acid and the spectrum of UO_2OH^+ were used for spectra deconvolution. The spectrum of UO_2OH^+ was measured at a pH of 4.2 and a delay time of 10 µs after the laser pulse. Contributions of the single-species emissions to the measured multi-component spectra were calculated using mixing coefficients. The mixing coefficients were fitted to obtain a least-square error between the measured spectra and the sum of all single component spectra.

3. Results

The fluorescence spectra of the aqueous uranyl(VI) ion, shown in Fig. 1, reflects the symmetrical vibration of the U–O bond. The observed emission bands correspond to the electronic transitions $S_{11} \rightarrow S_{00}$ (473 nm) and

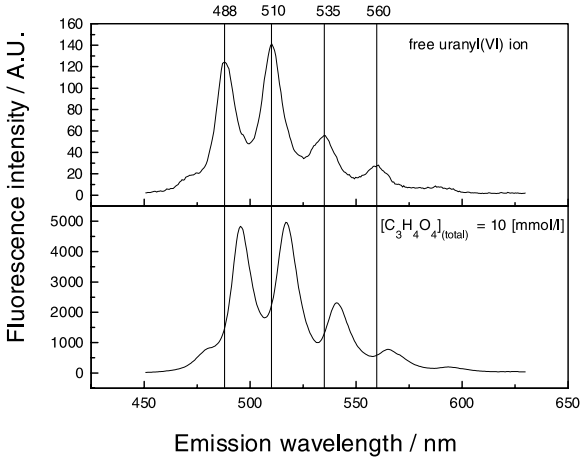

Fig. 1. Comparison of fluorescence spectra of the free UO_2^{2+} aquo ion and the uranyl(VI) spectrum at excess malonate concentration ($[UO_2^{2+}]_{(total)} = 5 \times 10^{-6}$ M; pH = 4; $I = 0.1$ M).

$S_{10} \rightarrow S_{0\nu}$ with $\nu = 0$–4 (488 nm, 510 nm, 535 nm, 560 nm and 587 nm; [26] and [27]). The average vibronic splitting energy of the $S_{10} \rightarrow S_{0\nu}$ transitions in our measurement is $\nu_s = 864 \pm 22\ cm^{-1}$ (1σ) and agrees well with the literature value of $\nu_s = 860\ cm^{-1}$ [27].

With increasing malonate concentration a bathochromic shift of the uranyl(VI) emission takes place and is attributed to a uranyl(VI)–malonate complexation. The strongest shift was observed at a high relative malonate concentration and reaches a maximum of 7 nm (see Fig. 1). Additionally, a strong enhancement of the fluorescence intensity and an increased fluorescence lifetime occurs when the malonate ligand is present.

The evaluation of the integrated fluorescence intensities as a function of time show two decay components with fluorescence lifetimes different from $UO_2^{2+}{}_{(aq)}$, indicating the formation of uranyl(VI) malonate complexes. A typical biexponential fluorescence decay function is presented in Fig. 2. As described above, the deconvolution of the measured spectra using the program POLYLIFE allows the separation of the single-species spectra and the extraction of the fluorescence decay constants as a function of the emission

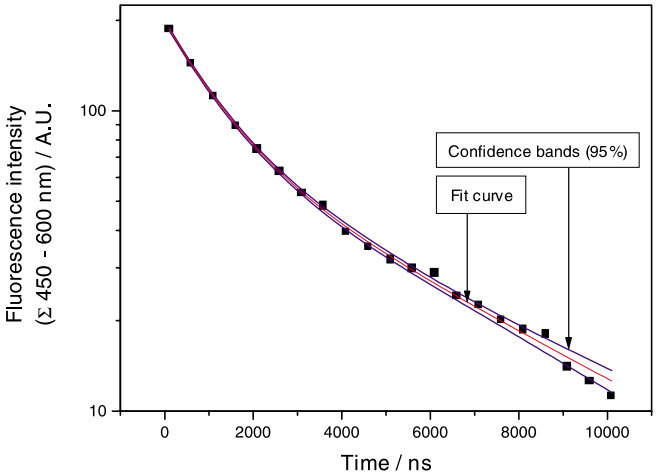

Fig. 2. Least-square fit of biexponential fluorescence decay according to Eq. (1). (Integrated fluorescence signal from 450 nm to 600 nm; $[C_3H_4O_4]_{(tot.)} = 5.0 \times 10^{-4}$ M.)

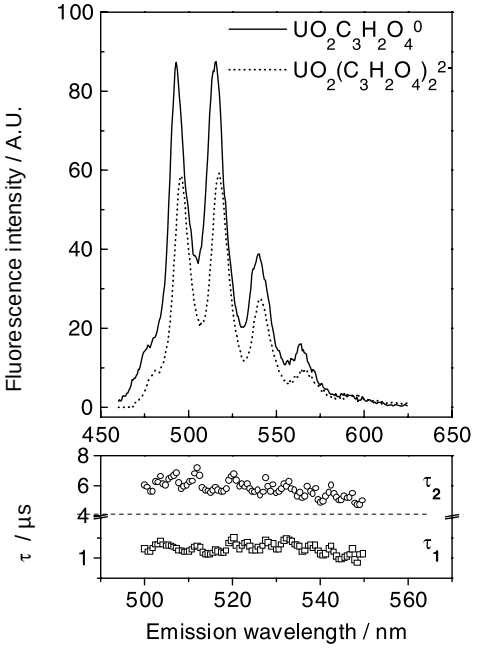

Fig. 3. Fluorescence decay constants and separated single spectra ($[C_3H_4O_4]_{(tot.)} = 5.0 \times 10^{-4}$ M; $\tau_1 = 1.14 \pm 0.01$ µs, $\tau_2 = 6.68 \pm 1.97$ µs; errors (2σ) of $\tau_{1,2}$ are within plot symbols).

wavelength. In Fig. 3 the results of the POLYLIFE calculation for the sample with $[C_3H_4O_4]_{(tot.)} = 5.0 \times 10^{-4}$ M are shown. We observe two spectra which are significantly different from the uranyl(VI) aquo ion and also do not match the spectrum of the species UO_2OH^+. Compared to the free uranyl(VI) aquo ion the emission of the first uranyl(VI) malonate complex is shifted for ~ 5 nm and ~ 7 nm for the second uranyl(VI) malonate complex. However, the typical vibronic splitting of the uranyl(VI) aquo ion emission remains.

The fluorescence decay constants of the first uranyl(VI) malonate complex and the uranyl(VI) aquo ion have similar values. However, the second uranyl(VI) malonate species possesses a fluorescence lifetime increased by a factor of ~ 4.

Fluorescence contributions of less than 10 percent cannot be resolved by the fitting procedure, especially if the fluorescence lifetime of the emitting species are similar. Therefore, only samples with high ligand excess ($> 2.5 \times 10^{-4}$ M total malonate) were used for the characterization of the uranyl(VI) malonate spectra and fluorescence lifetimes.

The emission bands were fitted with a mixed Gaussian–Lorentzian peak shape using the software GRAMS386™ (Galactic Industries Corporation, Salem, USA). In Table 2 the results are summarized together with the calculated fluorescence decay constants and equivalent parameters of the free uranyl(VI) ion and the first uranyl hydroxy species.

The calculated uranyl(VI) malonate spectra and the measured spectra of UO_2^{2+} and UO_2OH^+ were used to deconvolute the superimposed uranyl(VI) malonate spectra. To reduce statistical deviations of each individual spectrum resolved by the lifetime fit procedure, we obtained the characteristic spectra for the uranyl(IV) malonate species by averaging the corresponding spectra from all samples with a total malonate concentration $> 2.5 \times 10^{-4}$ M. The relative fluorescence contribution of the free uranyl(VI) ion to

Table 2. Emission band centers and FWHM (in parenthesis) and fluorescence lifetimes for uranyl malonates compared to UO_2^{2+} and UO_2OH^+.

Species	Peak 1 [nm]	Peak 2 [nm]	Peak 3 [nm]	Peak 4 [nm]	Peak 5 [nm]	Peak 6 [nm]	$\tau \pm 2\sigma$ [μs]
UO_2^{2+}	472 (10)	488 (19)	510 (12)	535 (15)	560 (14)	587 (20)	1.57 ± 0.06
UO_2OH^+	482 (14)	498 (15)	519 (17)	543 (22)	570 (25)	599 (19)	35 ± 2
$UO_2C_3H_2O_4^{\circ}{}_{(aq)}$	477 (10)	494 (11)	515 (13)	540 (12)	564 (18)	594 (15)	1.24 ± 0.02
$UO_2(C_3H_2O_4)_2^{2-}$	479 (9)	496 (11)	517 (11)	542 (12)	566 (18)	597 (15)	6.48 ± 0.02

the overall spectra decreases as a function of time due to the short fluorescence lifetime and comparatively low fluorescence yield. Therefore, we only used spectra measured after the first 200 ns delay step to deconvolute the spectra. A significant amount of $UO_2^{2+}{}_{(aq)}$ fluorescence was found for all samples. However, the UO_2OH^+ fluorescence intensity did not exceed the residues of the deconvoluted spectra. This indicates the insignificant concentration of the species UO_2OH^+ present in our samples. Consequently, the species UO_2OH^+ was excluded from all further data evaluation. A typical result of a deconvoluted spectrum is shown in Fig. 4.

The linear relationship between uranium concentration and fluorescence intensity was investigated from 10^{-7} M to 10^{-4} M (Fig. 5). The linear calibration curve allows the determination of the free uranyl(VI) ion directly from spectra deconvolution results. Assuming that the fluorescence intensity of the uranyl(VI) malonate spectra depends linearly on their concentrations, the total fluorescence intensity of the mixed spectrum can be expressed by the following equation:

$$A_{\text{total}} = \sum_{a}^{n} A_{0,a}\, c_a\,, \tag{2}$$

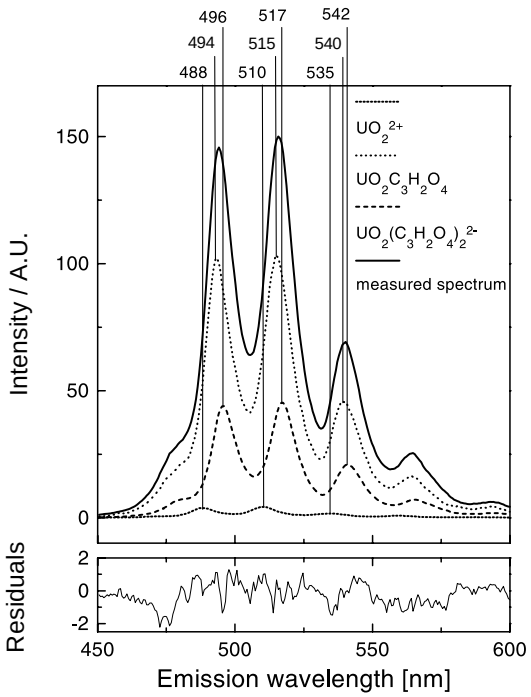

Fig. 4. Spectra deconvolution and fluorescence maxima for deconvoluted spectra ($[UO_2^{2+}]_{(\text{total})} = 5 \times 10^{-6}$ M; $[C_3H_4O_4]_{(\text{tot.})} = 10^{-3}$ M).

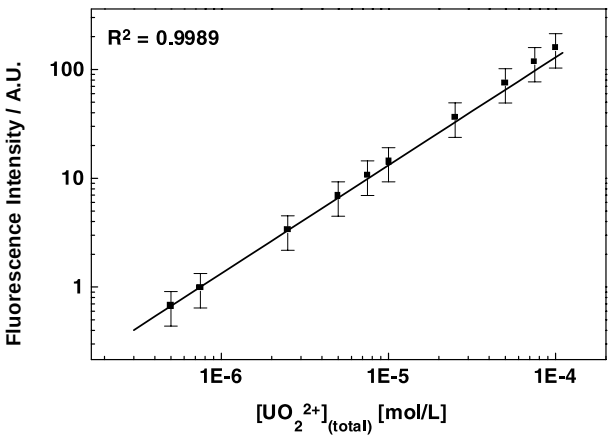

Fig. 5. Integrated fluorescence intensity (450–600 nm) as a function of total uranyl concentration ($I = 1$ M $HClO_4$).

with A_{total}: total fluorescence intensity of the multicomponent spectrum,
$A_{0,a}$: total fluorescence intensity of species a,
c_a: concentration of species a,
n: number of species contributing to A_{total}.

The concentrations for the uranyl(VI) malonate species were obtained by a least-square algorithm, minimizing the sum of squared errors of the uranium mass balance. The mass balance is given by (3):

$$[UO_2^{2+}]_{(\text{total})} = [UO_2^{2+}]_{(\text{free})} + [UO_2C_3H_2O_4^{\circ}{}_{(aq)}] + [UO_2(C_3H_2O_4)_2^{2-}]\,. \tag{3}$$

The mass was calculated from the fluorescence intensity for each species using Eq. (2). The calculated and analytical uranium concentration agreed within three percent or less. This confirms the assumption of a linear relationship between the fluorescence intensity and the concentration of each species.

Corresponding to uranyl(VI) malonate speciation models proposed in the literature [16–19], a complexation model of 1 : 1 and 1 : 2 metal to ligand ratio was formulated:

$$UO_2^{2+} + C_3H_2O_4^{2-} \Leftrightarrow UO_2C_3H_2O_4^{\circ}{}_{(aq)}\,, \tag{4}$$

$$UO_2C_3H_2O_4^{\circ}{}_{(aq)} + C_3H_2O_4^{2-} \Leftrightarrow UO_2(C_3H_2O_4)_2^{2-}\,, \tag{5}$$

$$UO_2^{2+} + 2C_3H_2O_4^{2-} \Leftrightarrow UO_2(C_3H_2O_4)_2^{2-}\,. \tag{6}$$

The stability constants are calculated using the following equations:

$$\beta_1 = \frac{[UO_2C_3H_2O_4^{\circ}{}_{(aq)}]}{[UO_2^{2+}]\cdot[C_3H_2O_4^{2-}]}, \quad (7)$$

$$K_2 = \frac{[UO_2(C_3H_2O_4)_2^{2-}]}{[UO_2C_3H_2O_4^{\circ}{}_{(aq)}]\cdot[C_3H_2O_4^{2-}]} \quad (8)$$

$$\beta_2 = \frac{[UO_2(C_3H_2O_4)_2^{2-}]}{[UO_2^{2+}]\cdot[C_3H_2O_4^{2-}]^2} \quad \text{or} \quad \beta_2 = K_2 + \beta_1 . \quad (9)$$

Because all experiments were conducted at pH 4, the incomplete malonic acid dissociation must be considered. The free ligand concentration was calculated using the following protonation equilibria:

$$K_1 = \frac{[C_3H_3O_4^-]\cdot[H^+]}{[C_3H_4O_4]}, \quad (10)$$

$$K_2 = \frac{[C_3H_2O_4^{2-}]\cdot[H^+]}{[C_3H_3O_4^-]}. \quad (11)$$

The 1 : 1 and 1 : 2 uranyl(VI) malonate complexation leads to the following mass balance equation for the total malonate concentration:

$$[C_3H_{4-x}O_4^{-x}]_{(total)} = [C_3H_4O_4] + [C_3H_3O_4^-] + [C_3H_2O_4^{2-}]_{(free)} + [UO_2C_3H_2O_4^{\circ}{}_{(aq)}] + 2[UO_2(C_3H_2O_4)_2^{2-}]. \quad (12)$$

The combination of Eqs. (3,8,10–12) gives Eq. (13), which is required to calculate the free ligand concentration in order to determine β_1 and β_2 (Eqs. (7) and (9)).

$$[C_3H_2O_4^{2-}] = \frac{\left\{\begin{array}{c} -K_1\cdot K_2\cdot(-[\,C_3H_{4-x}O_4^{-x})_{(total)} \\ +[UO_2C_3H_2O_4^{\circ}{}_{(aq)}] \\ +[\,UO_2C_3H_2O_4)_2^{2-}] \end{array}\right\}}{K_1\cdot K_2 + [H^+]\cdot K_2 + [H^+]^2}. \quad (13)$$

The dissociation constants of malonic acid given by Smith and Martell [28] were used after correction for an ionic strength of 0.1 M using the Davis equation [29] ($pK_1 = 2.74$, $pK_2 = 5.22$; $I = 0.1$ M).

Table 1 summarizes the calculated stability constants and the species concentrations derived from spectra deconvolution and Eq. (13). The validation of the postulated uranyl(VI) malonate complexation was performed by a linear regression analysis ([30, 31]). The general equation:

$$\beta = \frac{[UO_2(C_3H_2O_4)_y^{(2-2y)}]}{[UO_2^{2+}]_{(free)}\cdot[C_3H_2O_4^{2-}]^y} \quad (14)$$

was rearranged and transformed into a linear expression:

$$\log\frac{[UO_2(C_3H_2O_4)_y^{(2-2y)}]}{[UO_2^{2+}]_{(free)}} = y\cdot\log[C_3H_2O_4^{2-}] + \log\beta_y . \quad (15)$$

The slope y represents the metal to ligand ratio and indicates the correctness of the applied complexation model. Fig. 6 shows the linear regression analysis for 1 : 1 and 1 : 2 uranyl(VI) malonate complexation.

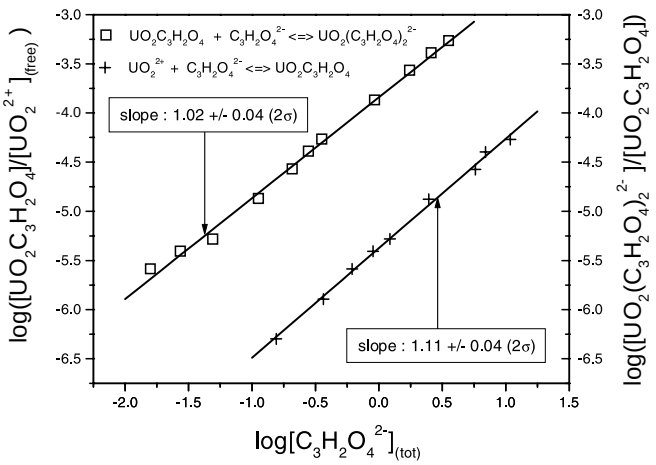

Fig. 6. Validation of uranyl(VI) malonate complexation by linear regression analysis.

4. Discussion

Fluorescence parameters

The fluorescence lifetime and the position of the emission bands assigned to the free uranyl(VI) ion are in good agreement with literature data for 0.1 M perchloric media ([1, 32–34]). For the system $UO_2^{2+}/C_3H_4O_4/H_2O$ no published fluorescence data are available. The positions of uranyl(VI) malonate emission bands are significantly different from those for the free uranyl(VI) ion and uranyl(VI) hydroxide species. However, the calculated fluorescence decay constants of the species $UO_2C_3H_2O_4^{\circ}{}_{(aq)}$ and UO_2^{2+} are similar.

The average vibronic splitting energy of the $UO_2C_3H_2O_4^{\circ}{}_{(aq)}$ and $UO_2(C_3H_2O_4)_2^{2-}$ spectrum is $\nu_s = 852 \pm 27\ cm^{-1}$ (1σ) and $\nu_s = 852 \pm 31\ cm^{-1}$ (1σ), respectively. The difference from the ν_s value of the uranyl(VI) aquo ion is insignificant. We conclude that the typical linear uranyl(VI) ion structure is not impacted by the ligand and the complexation takes place in the equatorial plane. This assumption is supported by results obtained by EXAFS measurements of uranyl(VI) complexes with carboxylic ligands [35].

The fluorescence intensity of the first uranyl(VI) malonate complex increased by a factor of 12 compared to the free uranyl(VI) aquo ion and by a factor of 48 for the second uranyl(VI) malonate complex. These values were calculated using (2), the integrated fluorescence intensity and the species concentrations.

A direct correlation between fluorescence intensities and fluorescence lifetimes could not be observed. Nevertheless, we attribute the increase in fluorescence intensity and fluorescence lifetime of the 1 : 2 uranyl(VI)–malonate complex to a reduced reactivity of the uranyl(VI) ion towards water as a fluorescence quencher due to malonate complexation.

Stability constants

The validation of uranyl(VI) malonate formation confirms the postulated complexation model and is depicted in Fig. 6 and the results are summarized in Table 3. The slope of the regression functions is 1.11 ± 0.04 (2σ) for the first and 1.04 ± 0.04 for second complexation reaction. The slope deviations from 1 can be explained by the existence of a minor

Table 3. Validation results for the postulated uranyl malonate complexation at 0.1 M ionic strength.

reaction	$\log \beta_1$ ($\pm 2\sigma$)	$\log \beta_2$ ($\pm 2\sigma$)	$\log K_2$ ($\pm 2\sigma$)	slope of regression function ($\pm 2\sigma$)	correlation coefficient R
I	5.36 ± 0.06	–	–	1.11 ± 0.04	0.99
II	–	9.20 ± 0.06	–	–	–
III	–	–	3.84 ± 0.04	1.04 ± 0.04	0.99

I: $[UO_2^{2+}] + [C_3H_2O_4^{2-}] \Leftrightarrow [UO_2C_3H_2O_4^{\circ}{}_{(aq)}]$
II: $[UO_2^{2+}] + 2[C_3H_2O_4^{2-}] \Leftrightarrow [UO_2(C_3H_2O_4)_2^{2-}]$
III: $[UO_2C_3H_2O_4^{\circ}{}_{(aq)}] + [C_3H_2O_4^{2-}] \Leftrightarrow [UO_2(C_3H_2O_4)_2^{2-}]$

Table 4. Literature data for complex stability constants of uranyl malonates, corrected to infinite dilution ($I = 0$).

$\log \beta^{\circ}{}_{x,y}$	pH	$[UO_2^{2+}]_{(total)}$ [M]	Ionic strength [M]	Temperature [°C]	Experimental method	Reference
4.38[a] 8.39[b]	2.5–3.5	5×10^{-3}	0.1	31	potentiometry	[16]
4.02[a] 7.75[b]	2–6.5	not published	0.2	30	potentiometry	[17]
4.76 ± 0.01[a] 8.76 ± 0.01[b]	2–5	8×10^{-4}–1.6×10^{-2}	1.0	25	potentiometry	[18]
4.52 ± 0.01[a] 8.58 ± 0.02[b]	not published	5×10^{-3}–2×10^{-2}	1.0	25	potentiometry	[19]
4.48 ± 0.06[a] 7.42 ± 0.06[b]	4	5×10^{-6}	0.1	23	TRLFS	this work

a: $[UO_2^{2+}] + [C_3H_2O_4^{2-}] \Leftrightarrow [UO_2C_3H_2O_4^{\circ}{}_{(aq)}]$;
b: $[UO_2^{2+}] + 2[C_3H_2O_4^{2-}] \Leftrightarrow [UO_2(C_3H_2O_4)^{2-}]$.

species which is impossible to resolve by TRLFS measurements. Due to the incomplete dissociation of malonic acid at a pH of 4, uranyl(VI) complexes with the first dissociation product may be possible. The attempt to include these complexation products into the data evaluation was made, but did not lead to meaningful results. A 5% analytical error for the species concentrations leads to a change of the determined complexation constants which is smaller than the given 2σ error. This also suggests that undetermined species do not exceed 5% of the mass balance.

Table 4 compares our stability constants with literature data. All published stability constants were corrected to infinite dilution using the Davies equation [29]. Our values agree well within their uncertainties with literature values obtained at much higher uranium concentrations than used in our study. Deviations are due to different experimental temperatures and slightly different dissociation constants used for malonic acid. The experiments from Athvale *et al*. [17] and Rajan and Martell [18] are performed under pH conditions from 2 to 6.5 and 2 to 5, respectively. Their proposed models show no appropriate consideration of uranyl(VI) hydroxide species which should not be neglected at the high total uranium concentrations used for potentiometric measurements.

5. Conclusions

Time-resolved laser-induced fluorescence spectroscopy is a sensitive tool to investigate the speciation of the uranyl(VI) malonate system at low concentrations. The TRLFS method allows to derive spectra arising from single species existent in a multicomponent system. The evaluation of time-resolved spectra as a function of emission wavelength permits the separation of superimposed spectral bands and gives the possibility to deduce single component spectra from a complex fluorescence signal. Stability constants of complex chemical systems can be easily calculated from TRLFS measurements.

References

1. Czerwinski, K. R., Buckau, G., Scherbaum, F., Kim, J. I.: Radiochim. Acta **65**, 111 (1994).
2. Kim, J. I., Czerwinski, K. R.: Radiochim. Acta **73**, 5 (1996).
3. Moulin, V., Laszak, I., Moulin, C., Decambox, P.: Report RCM 00794. TU München (1994).
4. Giesy, J. P., Geiger, R. A., Kevern, N. R.: J. Environ. Radioactivity **4**, 39 (1986).
5. Shanbhag, P. M., Choppin, G. R.: J. Inorg. Nucl. Chem. **43**(12), 3369 (1981).
6. Munier-Lami, C., Adrian, Ph., Berthelin, J., Rouliller, J.: Org. Geochem. **9**(6), 285 (1986).
7. Kribek, B., Podlaha, J.: Org. Geochem. **2**, 93 (1980).
8. Li, W. C., Victor, D. M., Chakrabartl, C. L.: Anal. Chem. **52**, 520 (1980).
9. Glaus, M. A., Hummel, W., Van Loon, L. R.: PSI Labor für Entsorgung. Report TM-44-94-04 (1994).
10. Rao, L., Choppin, G. R.: Radiochim. Acta **69**, 87 (1995).
11. Pinheiro, J. P., Mota, A. M., Simões Gonçalves, M. L.: Anal. Chim. Acta **284**, 525 (1994).
12. Kim, J. I., Buckau, G., Li, G. H., Duschner, H., Psarros, N.: Fresenius' J. Anal. Chem. **338**, 245 (1990).
13. Caceci, M. S.: Radiochim. Acta **39**, 51 (1985).
14. Thomason, J. W., Susetyo, W., Carreira, L. A.: Appl. Spectrosc. **50**/**3**, 401 (1996).
15. Dobbs, J. C., Susetyo, W., Knight, F. E., Castles, M. A., Carreira, L. A., Azartraga, L. V.: Anal. Chem. **61**, 483 (1989).

16. Ramamoorthy, S., Santappa, M.: Bull. Chem. Soc. Japan. **42**, 411 (1969).
17. Athavale, V. T., Mahadevan, N., Mathur, P. K., Sathe, R.: J. Inorg. Nucl. Chem. **29**, 1947 (1967).
18. Rajan, K. S., Martell, A. E.: J. Inorg. Nucl. Chem. **29**, 523 (1967).
19. Di Bernardo, P., Di Napoli, V., Cassol, A., Magon, L.: J. Inorg. Nucl. Chem. **39**, 1659 (1977).
20. Bartusek, M.: Coll. Czechoslov. Chem. Commun. **32**, 116 (1967).
21. Jahagirdar, D. V., Khanolkar, D. D.: J. Inorg. Nucl. Chem. **35**, 921 (1973).
22. Palaskar, N. G., Jahagirdar, D. V., Khanolkar, D. D.: J. Inorg. Nucl. Chem. **38**, 1673 (1976).
23. *Gmelins Handbuch der anorganischen Chemie*. Bd. 55, 8. Auflage, Weinheim und Berlin (1936) p. 136.
24. Geipel, G., Brachmann, A., Brendler, V., Bernhard, G., Nitsche, H.: Radiochim. Acta **75**, 199 (1996).
25. Brendler, V., Brachmann, A., Geipel, G.: Annual Report 1996, 13–14. Forschungszentrum Rossendorf e.V., Institute of Radiochemistry.
26. Bell, J. T., Biggers, R. E.: J. Molec. Spectrosc. **25**, 312 (1968).
27. Rabinowitsch, E., Belford, R. L.: *Spectroscopy and Photophysics of Uranyl Compounds*. Pergamon Press, Oxford (1964).
28. Smith, R. M., Martell, A. E.: NIST Critically selected stability sonstants of metal complexes. Database Version 2.0, U.S. Departement of Commerce, National Institute of Standards and Technology, Gaithersburg, MD, USA (1995).
29. Davies, C. W.: *Ion Association*. Butterworths, London (1962).
30. Connors, K. A.: *Binding constants, the measurements of molecular complex stability*. John Wiley & Sons, New York (1987).
31. Rossotti, F. J. C., Rossotti, H.: *The determination of stability constants*. McGraw-Hill Book Company, New York (1961).
32. Meinrath, G., Kato, Y., Yoshida, Z.: J. Radioanal. Nucl. Chem. **174**, No. 2, 299 (1993).
33. Kato, Y., Meinrath, G., Kimura, T., Yoshida, Z.: Radiochim. Acta **64**, 107 (1994).
34. Moulin, C., Decambox, P., Moulin, V., Decaillon, J. G.: Anal. Chem. **67**, 348 (1995).
35. Reich, T., Hudson, E. A., Denecke, M. A., Allen, P. G., Nitsche, H.: Structural analysis of uranium(VI) complexes by X-ray absorption spectroscopy. Poverkhnost **149**, 4 (1997).